chloride, 18704-37-5; cyclohexanol, 108-93-0; DL-menthone, 1074-95-9; *p*-nitrobenzoate, 117893-72-8; DL-neomenthol, 3623-51-6; 2-mercaptopyridine, 2637-34-5; 2-pyridinesulfonyl chloride, 66715-65-9; 3-pyridinesulfonyl chloride, 16133-25-8; 3-pyridinesulfonic acid, 636-73-7; dansyl chloride, 605-65-2; *trans*-4-*tert*-butylcyclohexanol, 21862-63-5; *exo*-norbornol, 497-37-0; L-menthol, 2216-51-5; 2-octanol, 123-96-6; 1-octanol, 111-87-5; cyclohexylmethanol, 100-49-2.

Structural and Complexation Properties of 2,11-Diselena[3.3](2,6)pyridinophane

Subramaniam Muralidharan,* Massoud Hojjatie,* Millicent Firestone, and Henry Freiser

Strategic Metals Recovery Research Facility, Department of Chemistry, University of Arizona, Tucson, Arizona 85721

Received June 15, 1988

2,11-Diselena[3.3](2,6)pyridinophane ($PyPySe_2$) has been synthesized in excellent yield by the high dilution method. Its conformational behavior in solution has been unambiguously determined by variable temperature (VT) ^1H, $^{13}C\{^1H\}$, and $^{77}Se\{^1H\}$ NMR. $PyPySe_2$ exists predominantly in the syn conformation, which undergoes flip of the pyridine rings and twist of the methylene bridges. The syn forms arising from pyridine flips cannot be distinguished by VT NMR as the energy barrier is low for this process. The syn forms arising from methylene twists can be differentiated by the nonequivalency of the bridge protons in VT NMR. The coalescence temperature for the bridge protons yields an activation barrier, $\Delta G^{\ddagger}$, of 37.4 kJ mol^{-1} for this process. The activation barrier for this process in the phenyl analogue is 30.4 kJ mol^{-1}. The difference in the activation barriers (7 kJ mol^{-1}) is due to the electrostatic interaction of the nitrogen lone pairs in the transition state of the methylene twist where the two pyridine rings are horizontal with respect to each other. $PyPySe_2$ complexed Ni^{2+} and Cu^{2+} in CH_3NO_2 with these complexes exhibiting similar stability constants, indicating that both metal ions fit equally well in the cavity of the heterophane. The stability constant values indicate a typical host–guest interaction. The X-ray structure determined from a single crystal of $[NiPyPySe_2(H_2O)_2][ClO_4]_2 \cdot CH_3NO_2$ belonging to the *Pnma* space group shows that the heterophane is in a syn conformation and highly symmetrical. This is in contrast to the Ni^{2+} complex of the thia analogue where the heterophane is distorted from the syn conformation. Interesting differences in the spectral and conductivity properties of the Cu(II) complex are observed when the coordinated H_2O is replaced by Cl^-. The heterophane and its metal and charge-transfer complexes are semiconductors at room temperature with the $CuPyPySe_2Cl_2$ complex exhibiting the best conductivity.

Introduction

Cyclophanes have attracted the attention of chemists for some time. Their synthesis, conformation, electronic structure, and host–guest chemistry have been the subjects of many investigations.[1] Heterophanes containing nitrogen, oxygen, and sulfur in the bridge have also been widely studied.[1] There have been, however, only a few reports of cyclophanes with selenium in the bridge.[2] Cyclophanes with selenium in the bridge are attractive for several reasons, namely, (1) selenium in the bridge provides an additional tool for the investigation of the conformational properties of the cyclophanes by ^{77}Se NMR [Such a tool is absent in the case of nitrogen, oxygen, and sulfur atoms in the bridge.], (2) selenium is more polarizable than nitrogen, oxygen, and sulfur, which could influence the complexation properties of selenacyclophanes with metal ions and charge-transfer complexation with electron acceptors like tetracyanoquinodimethane (TCNQ) and tetracyanoethylene (TCNE), and (3) the presence of selenium provides the possibility for novel conductivity properties of the cyclophanes and their complexes. We have initiated in our laboratory an investigation of the chemistry of selenacyclophanes for these reasons. We have synthesized 2,11-diselena[3.3](2,6)pyridinophane in >95% yields, characterized its conformational behavior by ^1H, $^{13}C\{^1H\}$, and $^{77}Se\{^1H\}$ NMR, investigated its complexation properties with transition-metal ions and electron acceptors, and determined the conductivity properties of these complexes. The crystal and molecular structure of its nickel(II) complex was also determined. This, to our knowledge, is the first report of the complexation and conductivity properties of selenacyclophanes.

Results and Discussion

The procedure we have adopted for the synthesis of $PyPySe_2$ provides >95% yield in comparison to the procedure used by Mitchell for the synthesis of 2,11-diselena[3.3]metacyclophane with xylylene bromide and Na_2Se, which gave the corresponding product in 7% yield.[10]

Conformational Properties of $PyPySe_2$. The conformational characteristics of metacyclophanes with and without heteroatoms in the bridge have been investigated in detail.[11] Relatively fewer investigations on the structurally analogous [3.3](2,6)pyridinophanes have been re-

(1) (a) *Cyclophanes*; Keehn, P. M., Rosenfeld, S. M., Eds.; Academic Press: New York, 1983; Vol. I and II. (b) *Topics in Current Chemistry*, Vogtle, F., Ed.; Springer-Verlag: Berlin, 1983; Vol. 113, pp 1–183. (c) *Topics in Current Chemistry*, Vogtle, F., Ed.; Springer-Verlag: Berlin, 1983; Vol. 115, pp 1–156.
(2) Higuchi, H.; Misumi, S. *Tetrahedron Lett.* **1982**, *23*, 5571.
(3) Beck, M. T. *Chemistry of Complex Equilibria*; Van Nostrand Reinhold Company: London, 1970; pp 86–92.
(4) Van der Pauw, L. J. *Philips Res. Rep.* **1958**, *13*, 1.
(5) Cromer, D. T.; Waber, J. T. *International Tables for X-Ray Crystallography*; The Kynoch Press: Birmingham, England, 1974; Vol. I, Table 2.2B.
(6) Ibers, J. A.; Hamilton, W. C. *Acta Crystallogr.* **1964**, *17*, 781.
(7) Cromer, D. T. *International Tables for X-Ray Crystallography*; The Kynoch Press: Birmingham, England, 1974; Vol. IV, Table 2.3.1.
(8) Cruickshank, D. W. J. *Acta Crystallogr.* **1949**, *2*, 154.
(9) Frenz, B. A. In *Computing in Crystallography*; Schenk, R., Olthof-Hazelkamp, R., VanKonigsceld, H., Bassi, G. C., Ed.; Delft University Press: Delft, Holland, 1978; pp 66–71.
(10) Mitchell, R. H. *Can. J. Chem.* **1980**, *58*, 1398.
(11) (a) Mitchell, R. H. In *Cyclophanes*; Keehn, P. M., Rosenfeld, S. M., Eds.; Academic Press: New York, 1983; Vol. I, pp 239–310. (b) Lai, Y. H. *Heterocycles* **1981**, *16*, 1739.

0022-3263/89/1954-0393$01.50/0

ported, however. Newkome has investigated the crystal structure of 2,11-dithia[3.3](2,6)pyridinophane and found this to exist in the syn conformation.[12] Low-temperature multinuclear NMR studies have not been reported on the dithia- or diselena[3.3]pyridinophanes to determine the nature of the solution species and the equilibrium involved. The low solubility of 2,11-diselena[3.3](1,3)phenylcyclophane was a problem for variable-temperature NMR studies.[13] The excellent solubility of 2,11-diselena[3.3](2,6)pyridinophane in chlorinated solvents allowed us to perform multinuclear, ^1H, $^{13}C\{^1H\}$, and $^{77}Se\{^1H\}$ NMR studies to understand its conformational properties in solution. Following the numbering scheme for cyclophanes indicated below, the chemical shifts of ^1H, ^{13}C, and ^{77}Se

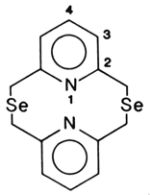

are listed in the Experimental Section under the preparation of $PyPySe_2$. The ^1H NMR chemical shifts are very similar to those reported by Newkome for the thia analogue.[12] By analogy, the predominant conformation of $PyPySe_2$ is syn. Variable-temperature ^1H NMR of $PyPySe_2$ in CD_2Cl_2 indicated that the bridge CH_2 protons and the pyridine protons remain singlets to 183 K. The CH_2 protons, however, exhibited gradual line broadening while the pyridine protons remained sharp singlets. At 182 K the CH_2 proton signals underwent splitting with the new peaks at 3.9 and 4.0 ppm. Variable-temperature $^{13}C\{^1H\}$ NMR exhibited no change in the shape of the bridge CH_2 or pyridine carbons from room temperature to 170 K, all peaks remaining sharp singlets. Similarly $^{77}Se\{^1H\}$ NMR of the bridge Se was invariant with temperature, remaining a singlet to 170 K. The transformation that is consistent with these variable-temperature NMR studies is the rocking motion of the bridge as shown below, originally suggested by Newkome.[12]

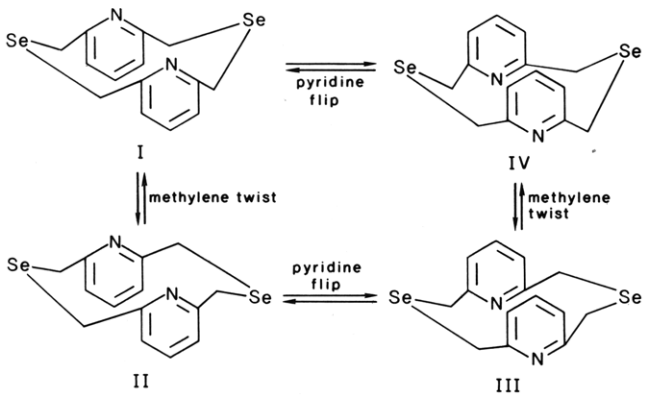

It is evident from the above that the barrier for the pyridine flip is not very high and the only way to distinguish two conformers obtained by pyridine flip is by $^{77}Se\{^1H\}$. This, in all likelihood, is practically impossible, as most solvents will freeze at a temperature where the pyridine flip could be slowed to the NMR time scale. The conformational change involving methylene twist, however, should have a higher barrier than that of the pyridine flip. The conformers obtained by methylene twist such as I and

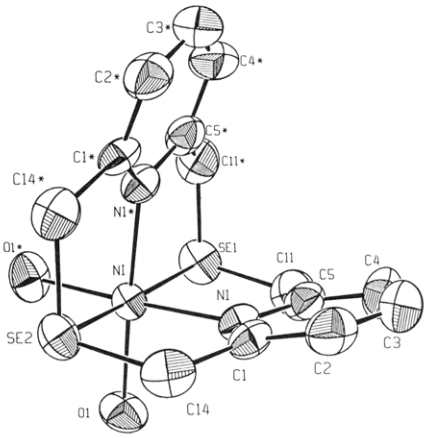

Figure 1. ORTEP drawing of $[NiPyPySe_2(H_2O)_2]^{2+}$ showing 50% probability of ellipsoids.

II appear to have nonequivalent bridge methylenes and seleniums but equivalent aromatic protons and equivalent carbons. The nonequivalency of the bridge seleniums is averaged by the pyridine flip, for example, the equilibrium II $\rightleftharpoons$ III. Thus, at the temperature where the CH_2 twist can be slowed, namely, 182 K as in the present case, two distinct signals are seen for the CH_2 protons, but a single signal is observed for the aromatic protons, bridge Se, and the C atoms. The coalescence temperature of 183 K for the CH_2 proton signals along with the NMR line width of 37.5 Hz yields $\Delta G^{\ddagger}$ for the methylene twist to be 37.4 kJ mol^{-1}.[14] We found that when one of the pyridines is replaced by phenyl to obtain 2,11-diselena[3.3](2,6)-pyridino(1,3)phenylcyclophane, the coalescence temperature for the methylene twist becomes 168 K, which yields a $\Delta G^{\ddagger}$ for this process of 33.9 kJ mol^{-1}. Thus the replacement of one pyridine by the corresponding phenyl lowered activation for the methylene twist by about 3.5 kJ mol^{-1}. This experiment allows us to estimate the $\Delta G^{\ddagger}$ for the phenyl analogue of $PyPySe_2$, namely, 2,11-diselena[3.3](1,3)phenylcyclophane, to be about 30.4 kJ mol^{-1}. The coalescence temperature for this compound based on the estimated $\Delta G^{\ddagger}$ is 150 K. It is interesting to note that the activation barrier for the methylene twist increases as the phenyl is replaced by pyridine or, specifically, the sp^2 carbon bearing hydrogen in the aromatic ring flanked by the two methylenes is replaced by sp^2 nitrogen with its lone pair. Examination of the methylene twist using space-filling models reveals a transition state in which the pyridine rings are horizontal with respect to each other, which increases the electrostatic interaction between the lone pairs on the nitrogen atoms. This electrostatic interaction accounts for the difference in the $\Delta G^{\ddagger}$ of 7 kJ mol^{-1} for the methylene twist between $PyPySe_2$ and its phenyl analogue. We are also in the process of resolving the crystal structure of the ligand $PyPySe_2$ to demonstrate that it exists predominantly in form I of the syn conformation as shown above.

Crystal Structure of $[NiPyPySe_2(H_2O)_2][ClO_4]_2 \cdot CH_3NO_2$. The bond distances and bond angles are given in Table II. The ORTEP diagram of the complex is shown in Figure 1. Nitromethane is present in the crystal lattice and not coordinated to Ni^{2+}. The unit cell has four each of $[Ni(PyPySe_2)(H_2O)_2][ClO_4]_2$ and CH_3NO_2.

It is evident from Figure 1 that the ligand is extremely symmetrical and Ni^{2+} selectively complexes with syn conformer I. This symmetry was exploited in the resolu-

(12) Newkome, G. R.; Pappalardo, S.; Fronczek, F. R. *J. Am. Chem. Soc.* **1983**, *105*, 5152.
(13) Mitchell, R. H. *Can. J. Chem.* **1980**, *58*, 1398.
(14) Gunther, H. *NMR Spectroscopy*; Wiley: New York, 1980; pp 240–244.

tion of X-ray data, generating one-half of the complex containing Ni, a H_2O, the bridge Se's, a bridge CH_2, and a pyridine, and the other half being generated by a reflection of this half about the mirror plane containing the two selenium atoms and Ni. The atoms in the half of the molecule generated in this fashion are indicated by an asterisk in Figure 1. It is not surprising that conformer I is able to selectively complex Ni^{2+} as this conformation presents a cavity in which the pyridine nitrogens and bridge seleniums can readily coordinate to Ni^{2+}. The cavity in the other conformers does not have the favorable disposition of all the N and Se to coordinate to the Ni^{2+}.

The Ni^{2+} complex of the thia analogue, namely, $PyPyS_2$, has been prepared as the chloride complex by Lewis and its crystal structure determined.[15] Comparing the crystal structures of $Ni(PyPyS_2)Cl_2$ and $[Ni(PyPySe_2)(H_2O)_2][ClO_4]_2$, we find that the latter complex is more symmetric than the former, where the Ni^{2+} is still complexed by the macrocycle in the syn conformation I, which is distorted. $PyPySe_2$ is less distorted upon complexation with Ni^{2+} than $PyPyS_2$ because Ni^{2+} fits in the cavity defined by the heteroatoms better in the former than in the latter. Larger cavity size in $PyPySe_2$ is due to the larger covalent radius of Se compared to S and longer C–Se distance. The Se1–Ni–Se2 angle of 171.3°, which is closer to the ideal value of 180° compared to the S1–Ni–S2 angle of 163.7°, is an indication of the differences in the size of the cavity in the two macrocycles. The N1–Ni–N1 angle in the $PyPySe_2$ complex is 84.2°, compared to the same angle in $PyPyS_2$ which is 88.2°. The Se1–Ni–Se2 and N1–Ni–N1 angles indicate that the cavity in $PyPySe_2$ adjusts its size to fit Ni^{2+} tightly by the simultaneous movement of the bridge heteroatom and the pyridine rings. The covalent radii of Se and S differ by 0.14 Å, but the Ni–Se and Ni–S distances differ by only 0.072 Å, indicating movement of the bridge Se toward the Ni^{2+} in the cavity to attain a tight fit of the metal ion. The difference in the bridge C–Se and C–S distances, namely, C11–Se1 and C11–S1 bond distances, is 0.08 Å, less than the covalent radii difference of Se and S, indicating that the C–Se bond in $PyPySe_2$ is stronger than expected on the basis of the covalent radius of Se. The difference between the Ni–O distance of 2.073 Å in the $PyPySe_2$ complex and the Ni–Cl distance of 2.363 Å in the $PyPyS_2$ complex is entirely accounted for by the difference in the covalent radii of Cl and O, which is 0.26 Å. The average values of C–C and C–N bond distances of the pyridine ring in the $PyPySe_2$ complex are 1.37 Å and 1.35 Å. The corresponding values in the $PyPyS_2$ complex are 1.38 Å and 1.35 Å. The average values of C–C–C, C–N–C, and N–C–C bond angles of the pyridine rings in the $PyPySe_2$ complex are 119.4°, 117.8°, and 121.9°. These values in the $PyPyS_2$ complex are 119.1°, 118.7°, and 122°, respectively. Thus the bond distances and bond angles of the pyridine rings in the two complexes are essentially the same, given the errors encountered in the refinement of X-ray structure data.

Complexation and Conductivity Behavior. The stability constants of the metal complexes in CH_3NO_2 are listed in Table I. The UV–vis spectra are shown in Figure 2. These spectra indicate that, both in the case of Ni(II) and Cu(II), we are dealing with typically octahedral complexes.[16]

It is interesting to note that the stability constants of the three metal complexes are very similar and not very large, indicating a typical host–guest interaction between the metal ion and the macrocycle with the metal ion entering the cavity of the cyclophane. Based on the X-ray structure of the Ni(II) complex of $PyPySe_2$, it is obvious that Ni(II) and Cu(II) should fit equally well in the cavity of the heterophane, which might explain the similar values for stability constants. Very few determinations of the stability constants of metal ion complexes of heterophanes have been reported in the literature. The stability constant for the complexation of Ag(I) by a cyclophane (not heterophane) in CH_3OD is 1.95×10^2 M^{-1}.[17] Considering the differences in the solvents used and the fact that Ag(I) is a second row transition metal, this stability constant is not very different from the ones we have determined. One might have expected a larger value for stability constants for the $PyPySe_2$ complexes of transition metals given the coordination of N and Se and, as a result, complexes stronger than a typical host–guest interaction.

Table I. Formation Constants K and Specific Conductance ρ of 1:1 Complexes of 2,11-Diselena[3.3](2,6)pyridinophane at 25 °C

complex	λ,[a] nm	K, M^{-1}	ρ,[d] Ω^{-1} cm^{-1}
$[NiPyPySe_2(H_2O)_2][ClO_4]_2$	858[b]	$(2.8 \pm 0.06) \times 10^3$	5.3×10^{-3}
$[CuPyPySe_2(H_2O)_2][ClO_4]_2$	436[b]	$(4.5 \pm 1.5) \times 10^3$	3.1×10^{-3}
$CuPyPySe_2Cl_2$	432[b]	$(1.6 \pm 0.1) \times 10^4$	4.6×10^{-2}
$PyPySe_2$–TCNQ	640[c]	42.2 ± 1.6	1.4×10^{-6}
$PyPySe_2$–TCNE	525[c]	49.8 ± 2.5	

[a] For K determination. [b] In CH_3NO_2. [c] In $CHCl_3$. [d] As pressed pellets. ρ of $PyPySe_2 = 2.1 \times 10^{-5}$ Ω^{-1} cm^{-1}.

There are some interesting differences between the aquo and chloro Cu(II) complexes. In the UV–vis spectra, the band in the 600–700-nm region in these complexes contains the metal d–d transition and the Se(π) → Cu(d) charge-transfer transition. The peak in the 400-nm region is due to Se(σ) → Cu(d) transition based on the assignment for certain Cu(II)–S_2N_2 macrocyclic complexes made by Woodruff.[18] For the chloro complex both peaks are red-shifted with the longer wavelength peak exhibiting a much larger shift than the shorter wavelength peak. The molar absorptivities for the peaks in the chloro complex are also higher by as much as a factor of 2 for the longer wavelength peak. The chloro complex has $2Cl^-$ occupying the 5th and 6th coordination sites, while in the aquo complex these are occupied by H_2O. As Cl^- is a stronger ligand than water in the spectrochemical series, it brings the e_g orbitals of Cu(II) closer in energy to the Se(π) orbitals by greater ligand field stabilization, thus lowering the energy for Se(π) → Cu(d) transition. The perturbation on the Se(σ) → Cu(d) transition, while in the same direction, is not as large, indicating that the σ and π levels of the macrocycle also move relative to the e_g orbitals. The chloro complex is roughly 3 times more stable than the aquo complex due to the influence of the Cl^- coordination.

We observed differences in the solid-state as well as solution EPR spectra of the chloro and aquo complexes of Cu(II). The solid-state EPR spectra of the two complexes are typical of the rhombic system with the chloro complex exhibiting g values of $g_1 = 2.243$, $g_2 = 2.042$, $g_3 = 2.189$, and the aquo complex exhibiting g values of $g_1 = 2.141$, $g_2 = 2.051$, and $g_3 = 2.108$. The EPR in CH_3NO_2 has only one g value, as the tumbling motion in the solu-

(15) Constable, E. C.; Lewis, J.; Marquez, V. E.; Raithby, P. R. *J. Chem. Soc., Dalton Trans.* **1986**, 1747.
(16) Lever, A. B. P. *Inorganic Electronic Spectroscopy*, 2nd ed.; Elsevier: Amsterdam, 1984; pp 507–511, 554–560.
(17) Pierre, J. L.; Baret, P.; Chautemps, P.; Armand, M. *J. Am. Chem. Soc.* **1981**, *103*, 2986.
(18) Ferries, N. S.; Woodruff, W. H.; Rorabacher, D. B.; Jones, T. E.; Orchrymowycz, L. A. *J. Am. Chem. Soc.* **1978**, *100*, 168.

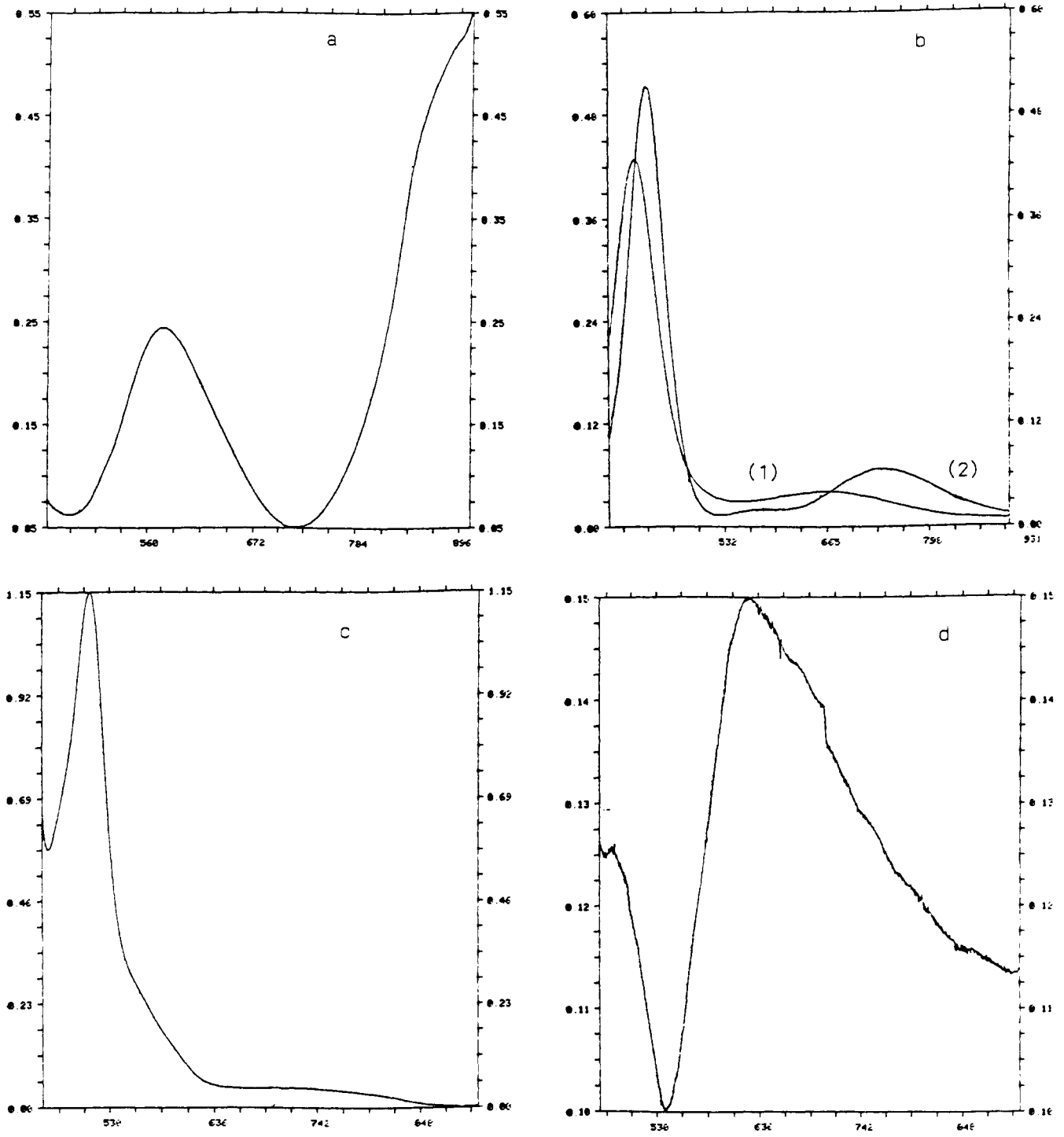

Figure 2. Uv–vis (A vs λ, nm, 1-cm cell) spectra of (a) $[NiPyPySe_2(H_2O)_2][ClO_4]_2$ (0.01 M) in CH_3NO_2, (b) (1) $[CuPyPySe_2(H_2O)_2][ClO_4]_2$ and (2) $CuPyPySe_2Cl_2$, 1.5×10^{-4} M of each in CH_3NO_2, (c) $PyPySe_2$–TCNE charge-transfer complex, 0.03 M in $CHCl_3$, and (d) $PyPySe_2$–TCNQ charge-transfer complex, 10^{-3} M in $CHCl_3$.

tion averages the g values. The chloro complex exhibited $g_{average} = 2.068$ with the hyperfine splitting constant $A_0 = 73.3$ gauss. The corresponding values for the aquo complex are $g_{average} = 2.102$ and $A_0 = 73.3$ gauss. The standard one-electron reduction potential for the aquo complex in CH_3CN with respect to the Ag/Ag^+ electrode is 0.15 V, with the complex exhibiting an almost reversible wave. The chloro complex exhibited two almost reversible waves, each corresponding to one-electron reduction, one at 0.15 V like the aquo complex and the other at 0.5 V. It was evident from the behavior of the waves of the two complexes that some decomposition of the Cu(I) complex occurs. The spectral and electrochemical behavior of the chloro complex is similar to the behavior of certain binuclear Cu(II) complexes with stacked coordination units with weak to moderately strong interaction between the Cu(II) sites.[19] In $CuPyPySe_2Cl_2$, interaction between the monomer units through the Cl^- ligand is possible leading to the equilibrium $2CuPyPySe_2Cl_2 \rightleftharpoons [CuPyPySe_2Cl_2]_2Cl_2$ in solution. Conductivity studies in CH_3CN and CH_3NO_2 to determine this equilibrium were inconclusive due to the low solubility of this complex. Such an equilibrium would

(19) Kida, S.; Okawa, H.; Nishida, Y. In *Copper Coordination Chemistry: Biochemical and Inorganic Perspectives*; Karlin, K. D., Zubieta, J., Eds.; Academic Press: New York, 1983; pp 430–433.

Table II. Bond Distances and Bond Angles of $[NiPyPySe_2(H_2O)_2][ClO_4]_2 \cdot CH_3NO_2$[a]

atom 1	atom 2	distance	atom 1	atom 2	distance
		Bond Distances in Angstroms			
Se1	Ni	2.479 (2)	C1	C14	1.53 (1)
Se1	Ni	2.479 (2)	C2	C3	1.36 (1)
Se1	C11	1.907 (9)	C3	C4	1.38 (1)
Se1	C11	1.907 (9)	C4	C5	1.38 (1)
Se2	Ni	2.477 (2)	C5	C11	1.49 (1)
Se2	Ni	2.477 (2)	Cl20	O21	1.391 (6)
Se2	C14	1.914 (8)	Cl20	O22	1.365 (8)
Se2	C14	1.914 (8)	Cl20	O23	1.371 (7)
Ni	O1	2.073 (5)	Cl20	O24	1.347 (8)
Ni	O1	2.073 (5)	N30	O31	1.16 (1)
Ni	N1	2.082 (6)	N30	O31	1.16 (1)
Ni	N1	2.082 (6)	N30	O32	1.18 (1)
N1	C1	1.320 (9)	N30	O32	1.18 (1)
N1	C5	1.367 (9)	N30	C33	1.44 (2)
C1	C2	1.36 (1)	N30	C33	1.44 (2)

atom 1	atom 2	atom 3	angle	atom 1	atom 2	atom 3	angle
			Bond Angles in Degrees				
Ni	Se1	C11	92.1 (2)	Ni	N1	C5	118.7 (5)
Ni	Se1	C11	92.1 (2)	C1	N1	C5	117.8 (7)
C11	Se1	C11	100.5 (6)	N1	C1	C2	122.9 (8)
Ni	Se2	C14	92.1 (2)	N1	C1	C14	117.2 (7)
Ni	Se2	C14	92.1 (2)	C2	C1	C14	119.9 (7)
C14	Se2	C14	98.4 (5)	C1	C2	C3	120.5 (9)
Se1	Ni	Se2	171.33 (7)	C2	C3	C4	117.8 (9)
Se1	Ni	O1	92.6 (2)	C3	C4	C5	120.0 (9)
Se1	Ni	O1	92.6 (2)	N1	C5	C4	120.9 (8)
Se1	Ni	N1	87.2 (2)	N1	C5	C11	119.1 (8)
Se1	Ni	N1	87.2 (2)	C4	C5	C11	120.0 (8)
Se2	Ni	O1	93.6 (2)	Se1	C11	C5	117.3 (6)
Se2	Ni	O1	93.6 (2)	Se2	C14	C1	117.6 (5)
Se2	Ni	N1	86.4 (2)	O21	Cl20	O22	108.4 (5)
Se2	Ni	N1	86.4 (2)	O21	Cl20	O23	106.7 (5)
O1	Ni	O1	90.0 (3)	O21	Cl20	O24	110.4 (6)
O1	Ni	N1	92.9 (2)	O22	Cl20	O23	111.8 (7)
O1	Ni	N1	177.1 (2)	O22	Cl20	O24	108.6 (6)
O1	Ni	N1	177.1 (2)	O23	Cl20	O24	110.9 (6)
O1	Ni	N1	92.9 (2)	O31	N30	O32	125 (1)
N1	Ni	N1	84.2 (4)	O31	N30	C33	120 (1)
Ni	N1	C1	121.7 (6)	O32	N30	C33	115 (1)

[a] Numbers in parentheses are estimated standard deviations in the least significant digits.

explain the perturbation of the ligand energy levels observed in UV–vis spectra and a lower $g_{average}$ value in CH_3NO_2 due to weak interaction between the Cu(II) centers. The higher reduction potential in the cyclic voltammogram could be due to the reduction of the second Cu(II) center in this Cl^--bridged dimer. The macrocycle, free and complexed, exhibited an irreversible oxidation wave at 1.1 V in CH_3CN with respect to Ag/Ag^+, corresponding to the oxidation of Se in the bridge. This oxidation potential is about 0.4 V lower compared to those of simple disulfides like dibenzyl sulfide.[20] This could be due to the greater polarizability of Se compared to S and some interaction between the bridge Se atoms. Further comparisons with thiacyclophanes and organic selenides are not possible, as the oxidation potentials of these compounds have not been determined.

The formation constants for the charge-transfer complexes with TCNQ and TCNE complexes are similar and of the same order of magnitude compared to the TCNE complexes of some paracyclophanes.[21] It is again surprising that the presence of Se does not lead to stronger charge-transfer complexes. This indicates that very little polarization of the bridge selenium occurs and the charge-transfer complexation mainly involves polarization of the aromatic π electron density.

The conductivity data, Table I, indicate that the parent macrocycle and its complexes are semiconductors at room temperature with the metal complexes showing better conductivities than the parent macrocycle and its charge-transfer complex with TCNQ. Satisfactory data on the PyPySe–TCNE could not be obtained, as this yielded poor quality pellets for conductivity measurement. The fact that $CuPyPySe_2Cl_2$ has better conductivity than the aquo complexes of Cu(II) and Ni(II) indicates that it has a different crystal packing where the different stacks of the complex molecules interact better, possibly through Cl^- ligands, similar to the behavior of this complex in solution. The $PyPySe_2$–TCNQ complex is actually a poorer conductor than $PyPySe_2$ itself, indicating that the charge transfer from the macrocycle to TCNQ is not very efficient. The crystal lattice also could have irregular stacks of the charge-transfer complex, making electrical conductivity more difficult.

We have performed a number of interesting fundamental studies with the macrocycle 2,11-diselena[3.3]-(2,6)pyridinophane. We have characterized its conformational behavior and shown that it forms metal and charge-transfer complexes. The complexes are semiconductors at room temperature. Surprisingly, the presence of Se does not enhance the stability constants of the complexes or the conductivity of the TCNQ charge-transfer complex. This could be related to the high oxidation potential of the bridge Se, indicating that it is not easily polarized. We are extending our studies to other

(20) Cottrell, P. T.; Mann, C. K. *J. Electrochem. Soc.* **1969**, *116*, 1499.
(21) Mourad, A. E.; Eltamany, E. H.; Hopf, H. *Z. Phys. Chem. Leipzig* **1986**, *267*, 937–944.

pyridinophanes with substituents in the aromatic ring and bipyridinophanes to understand the structural factors that affect the Se potential and hence its polarizability.

Experimental Section

General Methods. Melting points were determined on an AcuLab melting point apparatus in open capillary tubes and are uncorrected. IR spectra were recorded on Perkin-Elmer Model 1800 FT-IR spectrometer. NMR spectra were measured with a Bruker WM-250 NMR spectrometer on samples containing tetramethylsilane as internal standard for ^1H and $^{13}C\{^1H\}$. $^{77}Se\{^1H\}$ NMR spectra were recorded with respect to dimethyl selenide as an external standard. Elemental analysis was performed by Galbraith Laboratories, Knoxville, TN.

All inorganic chemicals used in our studies were analytical grade. Inorganic chemicals were purchased from Alfa Products, Danvers, MA, and were 99% pure. Organic chemicals were purchased from Aldrich Chemical Co., Milwaukee, WI, and American Scientific Products, Phoenix, AZ, and were appropriately distilled or recrystallized.

2,6-Bis(selenocyanatomethyl)pyridine. This compound was prepared by the high dilution method by modifying the procedure of Misumi.[2] 2,6-Bis(selenocyanatomethyl)pyridine was prepared from 2,6-bis(bromomethyl)pyridine and KSeCN. To a stirred solution of 5.1 g (0.02 mol) of 2,6-bis(bromomethyl)pyridine in 150 mL of degassed acetone was added a solution of 7.2 g (0.05 mol) of KSeCN in 200 mL of degassed acetone dropwise under an argon atmosphere at room temperature over a period of 4 h. KBr was filtered off, and the solution concentrated to yield 5.8 g of 2,6-bis(selenocyanatomethyl)pyridine as pale yellow crystals (98%): mp 81 °C; ^1H NMR ($CDCl_3$) δ 4.46 (s, CH_2, $^2J_{SeH}$ = 16.7 Hz), 7.26 and 7.29 (d, 1:1, Ar*H*, J_{HH} = 7.8 Hz), 7.7, 7.73, and 7.76 (t, 1:2:1, Ar*H*, J_{HH} = 7.8 Hz); IR (KBr) ν(S–CN) 1650 cm^{-1}. Anal. Calcd for $C_9H_7Se_2N_2$: C, 35.9; H, 2.3; N, 9.3; Se, 52.5. Found: C, 35.8; H, 2.3; N, 9.4; Se, 52.0.

2,11-Diselena[3.3](2,6)pyridinophane. 2,6-Bis(selenocyanatomethyl)pyridine (1.5 g, 0.005 mol) and 2,6-bis(bromomethyl)pyridine (1.3 g, 0.005 mol) were each dissolved separately in a mixture of 80% freshly distilled peroxide-free THF and 20% absolute ethanol to a total volume of 200 mL and thoroughly degassed with Ar. They were added separately but simultaneously from two constant addition funnels over 20 h into 950 mL of freshly distilled peroxide-free THF and 50 mL of absolute ethanol containing an excess (1.5 g) of $NaBH_4$ at room temperature under Ar. The resulting solution was filtered and concentrated to dryness. The solid was treated with 100 mL of freshly distilled benzene. The benzene solution was evaporated to dryness to yield a white crystalline solid which was recrystallized from $CHCl_3$ (1.75 g, 96%): mp 121 °C; Anal. Calcd for $C_{14}H_{14}N_2Se_2$: C, 45.6; H, 3.8; N, 7.6; Se, 42.9. Found: C, 45.4; H, 3.7; N, 7.5; Se, 41.4. ^1H NMR ($CDCl_3$) δ 3.95 (s, CH_2, $^2J_{SeH}$ = 17.4 Hz), 6.87 and 6.9 (d, 1:1, H3, J_{HH} = 7.7 Hz), 7.12, 7.15, and 7.18 (t, 1:2:1, H4, J_{HH} = 7.7 Hz); $^{13}C\{^1H\}$ NMR ($CDCl_3$) δ 30.2 (s, CH_2, $^1J_{SeC}$ = 75.5 Hz), 120.7 (s, C3), 136.4 (s, C4), 157.8 (s, C2); $^{77}Se\{^1H\}$ NMR ($CDCl_3$) 358.2 (s, bridge Se).

Complexation of $PyPySe_2$ with Ni(II), Cu(II), TCNQ, and TCNE. The stoichiometry and stability constant of each complex were determined spectrophotometrically in a suitable solvent by Job's method by monitoring the absorbance of the given complex at an appropriate wavelength.[3] The results appear in Table I. The respective complexes were isolated in >95% yield by reacting the ligand with the given transition-metal salt or electron acceptor in the appropriate solvent. The preparation of the Ni(II) complex is described as a typical procedure. Sometimes mixtures of solvents were used when the complexes were prepared in large amounts for isolation. No solvent mixtures were used for the determination of stability constants.

2,11-Diselena[3.3](2,6)pyridinophane (0.5 g, 1.36×10^{-4} mol) was dissolved in 25 mL of $CHCl_3$ and purged with Ar. Nickel perchlorate hexahydrate (0.48 g, 1.36×10^{-4} mol) was dissolved in 100 mL of nitromethane and degassed with Ar. The Ni solution was added to the ligand solution under Ar and a purple solution resulted. The mixture was stirred at room temperature for 2 h and the solvents were then removed under vacuum to obtain the Ni(II) complex as a pale blue powder. Elemental analysis of the vacuum dried complex indicated it to be $[NiPyPySe_2][ClO_4]_2 \cdot CH_3NO_2$. Anal. Calcd: C, 26.22; H, 2.62; N, 6.12; O, 23.3; Cl, 10.33; Se, 23.01; Ni, 8.6. Found: C, 26.28; H, 2.68; N, 5.74; O, 23.42; Cl, 11.06; Se, 22.62; Ni, 8.94.

Molecular weight of the complex by vapor pressure osmometry in CH_3CN was 640 with the theoretical value being 686.6 for $[NiPyPySe_2][ClO_4]_2 \cdot CH_3NO_2$. With undried solvents, single crystals were grown from this sample by diffusing $CHCl_3$ into a nitromethane solution. As evident from the crystal structure, these crystals had the composition $[NiPyPySe_2(H_2O)_2][ClO_4]_2 \cdot CH_3NO_2$.

The Cu(II) complexes were prepared in a similar manner. The aquo complex was prepared by using $Cu(ClO_4)_2 \cdot 6H_2O$ and the chloro complex by using $CuCl_2 \cdot 2H_2O$. The aquo complex analyzed as $[CuPyPySe_2(H_2O)_2][ClO_4]_2$. Anal. Calcd: C, 25.2; H, 2.7; N, 4.2; O, 24.0; Cl, 10.6; Se, 23.7; Cu, 9.5. Found: C, 25.2; H, 2.8; N, 4; O, 24.7; Cl, 10; Se, 22.8; Cu, 9.8. The chloro complex analyzed as $CuPyPySe_2Cl_2$. Anal. Calcd: C, 33.4; H, 2.8; N, 5.6; Se, 31.4; Cl, 14.1; Cu, 12.7. Found: C, 33.7; H, 2.7; N, 5.4; Se, 30.9; Cl, 13.8; Cu, 12.5.

Conductivity Measurement on $PyPySe_2$ and Its Complexes. Room-temperature resistivities and, hence, conductivities of the ligand and its complexes were determined as pressed pellets by using the four-probe method of Van der Pauw.[4] Each sample (0.5 g) was dried under vacuum at room temperature for 3 h and pressed into a pellet with an IR pellet press at a pressure of 5000 psi. Contact was established between the stainless steel wires used as electrodes and the pellet by using the conductivity paste Electrodag 502 (Acheson Colloids Co., MI). The resistance of the pellet was measured from the voltage drop of a 1.5-V battery. The specific resistance was calculated from the measured resistance and thickness of the pellet.[4] The reciprocal of the specific resistance was taken as the specific conductance at room temperature. The results appear in Table I.

Cyclic Voltammetry Measurements. The one-electron reduction potentials of the aquo and chloro copper complexes and the one-electron oxidation potential of $PyPySe_2$ were determined at a Pt electrode in freshly distilled CH_3CN using 0.1 M $LiClO_4$ as supporting electrolyte and Ag/Ag^+ (0.1 M $AgNO_3$) as the reference electrode at room temperature (25 ± 1 °C). The potential was swept at 200 mv s^{-1} on a Princeton Applied Research Model 174A polarographic analyzer. Current vs potential plots were obtained on a Hewlett-Packard 7040A X-Y recorder.

Crystal Structure of $[NiPyPySe_2(H_2O)_2][ClO_4]_2 \cdot CH_3NO_2$. A light blue irregular crystal of dimension 0.54 × 0.45 × 0.25 mm of this complex was mounted on a glass fiber in random orientation on a Syntex-Nicolet P2 diffractometer. Preliminary examination and data collection were performed with Mo K_α (0.71073 Å) radiation on a Syntex $P2_1$ diffractometer without a monochromator. Cell constants and an orientation matrix for data collection were obtained from least-squares refinement, using the setting angle of 25 reflections in the range $20 < 2\theta < 29°$. The cell dimensions were a = 9.337 Å, b = 14.9617 Å, and c = 17.566 Å, with 4 molecules of the complex and 4 CH_3NO_2 per unit cell. The density of the crystal was determined by flotation in bromoform and hexane to be 2.01 with the calculated value being 1.96. The orthorhombic space group was determined to be *Pnma* (No. 62) from systematic absences and from the distribution of E values.

Intensity data were collected by using the $\theta/2\theta$ scan technique at 298 K over the range $0° < 2\theta < 50°$ at a rate of 2–8 °C min^{-1}. A total of 2505 reflections were collected, 2268 of which were unique and not systematically absent. After every 46 reflections, the intensities of 3 standard reflections were monitored. As these showed no significant variation during the experiment, no decay correction was applied. Lorentz and polarization corrections were applied to the data. An empirical absorption correction based on a series of ϕ-scan was applied to the data. Relative transmission coefficients ranged from 0.832 to 0.999 with an average of 0.936.

The structure was solved by direct method using MULTAN which provided 3 atoms. The remaining atoms were located in the following difference Fourier syntheses. The hydrogen atoms were added at idealized positions (C–H = 0.95 Å). Hydrogen atoms were included in the refinement but constrained to ride on the atom to which they were bonded.

The structure was refined in full-matrix least-squares, where the function minimized was $\sum w(|F_o| - |F_c|)^2$. The standard deviation of F^2, $\sigma(F^2)$, is defined by $\sigma(F^2) = [\sigma(I) + (pF^2)^2]^{1/2}$. The weights for each reflection were calculated by using the counter weighting scheme, $w = 4F^2/[\sigma(I) + (pF^2)^2]$, which reduced to w

$= 4F^2/\sigma^2(F^2)$ where the uncertainty factor, p, was set to the value of 0.04.

Scattering factors were taken from Cromer and Waber.[5] Anomalous effects were included in F_c for all non-hydrogen atoms.[6] The values for $\Delta F'$ and $\Delta F''$ were those of Cromer.[7] Only 1149 reflections with intensities greater than 3.0 times their standard deviation were used in the refinements. The final cycle of refinement included 169 variable parameters and converged with unweighted and weighted agreement factors of

$$R_1 = \sum||F_o| - |F_c||/\sum F_o = 0.05$$

$$R_2 = (\sum w(|F_o| - |F_c|)^2/\sum wF_o^2)^{1/2} = 0.054$$

The standard deviation of an observation unit weight was 1.73. There was one correlation coefficient greater than 0.5. The highest peak in the final difference Fourier had a height of 0.76 e/Å^3, with an estimated error base on $\sigma(F)$ of 0.13.[8] The minimum negative peak had a height of −0.55 e/Å^3, with an estimated error based on $\sigma(F)$ of 0.13. Plots of $\sum w(|F_o| - |F_c|)^2$ vs $|F_o|$, reflection order in data collection $\sin\theta/\lambda$, and various classes of indices showed no unusual trends. All calculations were performed on a VAX computer using SDP/VAX.[9]

Acknowledgment. The help provided by Dr. M. Bruck, Molecular Structure Lab, and Professor John H. Enemark, Department of Chemistry, University of Arizona, in solving the crystal structure of the nickel complex is gratefully acknowledged. Part of the crystal structure determination was a class project of Ms. Firestone in Chemistry 517. We also thank Professor Robert B. Bates for many helpful discussions.

Supplementary Material Available: Tables of additional positional parameters, bond distances, and bond angles for $[NiPyPySe_2(H_2O)_2][ClO_4]\cdot CH_3NO_2$ (5 pages); observed and calculated structure factors (6 pages). Ordering information is given on any current masthead page.

Concerning Model Metabolites of the Carcinogen 4-Nitroquinoline 1-Oxide. Reactivity and Solvolytic Behavior of 1-Hydroxy-4-(acetoxyimino)-1,4-dihydroquinoline

Martine Demeunynck,[†] Marie-France Lhomme,[†] John M. Mellor,[‡] and Jean Lhomme*,[†]

LEDSS, UA CNRS 332, Université Joseph Fourier de Grenoble, BP 53X, 38041 Grenoble Cedex, France, and Department of Chemistry, The University of Southampton, SO9 5NH Southampton, U.K.

Received April 19, 1988

1-Hydroxy-4-(acetoxyimino)-1,4-dihydroquinoline is obtained quantitatively by reaction of 1-acetoxy-4-(acetoxyimino)-1,4-dihydroquinoline with piperidine in dimethyl sulfoxide. Spectroscopic results establish that this monoacetate exists preferentially as a hydroxylamine tautomer rather than as an *N*-oxide in the pH range 2–9, but below pH 2 protonation affords the N-protonated ester and above pH 9 an anion is formed. Hydrolysis below pH 2 gives clearly 4-(hydroxyamino)quinoline 1-oxide, which is also the major hydrolysis product at pH >9. In the intermediate zone pH 2–9 the neutral acetate affords a variety of products, including those of substitution at the 3-position, via the breaking of the N–O bond. By study of the rate of solvolysis of the neutral acetate in different solvents, applying the Grunwald Winstein relation, and by comparison with the solvolysis of the model compounds 4-(acetoxyamino)quinoline and [[[(*p*-nitrophenyl)sulfonyl]oxy]amino]quinoline, it is concluded that for the latter solvolysis proceeds via the intermediacy of nitrenium ions. Similarly solvolysis of 1-hydroxy-4-(acetoxyimino)-1,4-dihydroquinoline gives nitrenium ion intermediates with enhanced rates attributed to the accelerating influence of the *N*-oxide functionality.

A number of derivatives of aromatic amines are known to be powerful carcinogens. It is generally recognized that their mode of action involves the ultimate carcinogen reacting in a covalent manner with DNA.[1] The exact nature of the ultimate carcinogens derived from these derivatives of aromatic amines has been an area of extensive study. Thus in investigations of derivatives of 2-aminofluorene, 4-aminobiphenyl, and 2-aminonaphthalene it has been established that products of oxidation, hydroxylamine derivatives, such as the *N*-acetyl-*N*-acetoxyamines, react with DNA bases.[2] It has been proposed that similar hydroxylamine derivatives are the reactive metabolites of mutagenic aromatic nitro compounds.[3] In particular 4-nitroquinoline 1-oxide (**1**), a powerfully carcinogenic compound, and its metabolites have received sufficient attention to be the subject of a recent review.[4] It is well established that initial enzymatic reduction can lead to the hydroxylamine **2**,[5] which exists preferentially as the hydroxyimino tautomer[6] $\mathbf{2_B}$. It has been proposed that these tautomers are further metabolized to compounds able to bind to nucleic acid bases. In support of this hypothesis the diacetate **3** has been shown in in vitro experiments to react with DNA and with nucleosides[7] to give small amounts of products by covalent attachment to the bases. In particular a product with deoxyguanosine has been

Scheme I

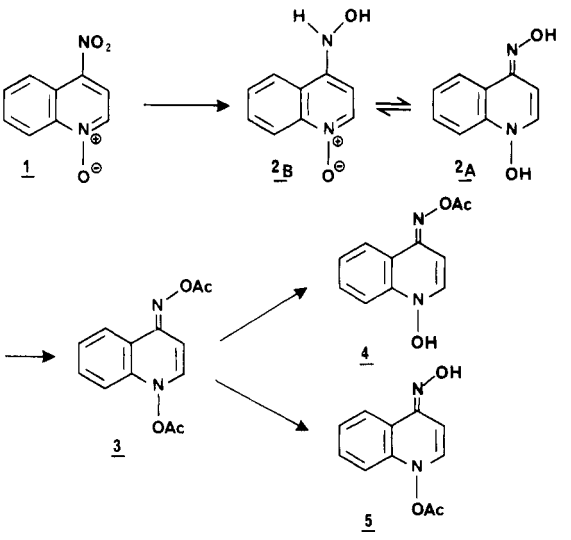

[†] Université Joseph Fourier–Grenoble.
[‡] The University of Southampton.

(1) Miller, J. A. *Cancer Res.* **1970**, *30*, 559.

0022-3263/89/1954-0399$01.50/0